J. Fluid Mech. (1995), *vol.* 282, *pp.* 115–129

Effect of polymer additives on Görtler vortices in Taylor–Couette flow

By S. H.-K. LEE†, S. SENGUPTA AND T. WEI

Department of Mechanical and Aerospace Engineering, Rutgers University, Piscataway, NJ 08855-0909, USA

(Received 23 June 1993 and in revised form 27 June 1994)

Taylor–Couette flow is ideal for studying drag-reducing polymer additives because, unlike turbulent boundary layers, the instabilities are better understood. Video records of laser-induced fluorescence experiments with and without polymers will be presented. Polyethylene-oxide (PEO) 'oceans' were used in concentrations of 20 and 100 p.p.m. In the Taylor number range, $3 \times 10^4 \leqslant Ta \leqslant 10^8$, Newtonian flow consisted of Taylor vortices which span the gap between cylinders and much smaller Görtler vortices at the inner cylinder wall. Measurements of core-to-core separation between counter-rotating vortices were made to estimate the Görtler instability wavenumber. These measurements show that PEO addition increases the Görtler wavenumber for a given Taylor number. At the lower Taylor numbers, Görtler vortex formation was suppressed by PEO. This implies that polymers directly affect the evolution of centrifugal instabilities.

1. Introduction

In this paper, the problem of how polymer molecules can interact with near-wall streamwise vortices to yield drag reduction is addressed. The traditional approach to drag reduction research is to study a particular turbulent flow with and without additives and look for differences in statistical quantities and coherent structure. The problem with this approach is that the instabilities responsible for regeneration of turbulence have not yet been definitively identified, let alone understood. This makes it difficult, if not impossible, to draw definitive conclusions on how polymers reduce drag.

An alternative approach was taken in this investigation. A flow was examined where the stability mechanisms were more clearly understood, making it possible to determine whether or not polymer additives affect the growth and roll-up of a specific instability. Specifically, the hypothesis that polyethylene-oxide (PEO) inhibits evolution of Görtler instabilities was examined.

In order to provide a context for this work, it is important to review literature on both polymer drag reduction and Taylor–Couette flows. Of particular relevance to this investigation are works on polymer molecule dynamics in drag reduction. This is still a wide open issue and a number of representative papers are cited here. For a more general review, the reader is referred to Wei & Willmarth (1992). The remainder of this introduction is devoted to discussion of stability of Taylor–Couette flow.

† Present address: Mechanical Engineering Department, University of Hong Kong Institute of Science and Technology, (UHKIST) Hong Kong.

1.1. *Definitions*

Before proceeding, it is necessary to note that there are a number of definitions of Taylor number, *Ta*, commonly in use. In this paper, *Ta* will be defined as

$$Ta = R_{in}\Omega^2 d^3/\nu^2 = (U_{in}^2 d^2/\nu^2)(d/R_{in}) = (Re_d^2)(d/R_{in}), \tag{1}$$

where R_{in}, R_{out} are the inner and outer cylinder radii, respectively, Ω is the inner cylinder angular velocity, $d = R_{out} - R_{in}$ is the gap width, ν is the kinematic viscosity (in this case of water), $U_{in} = R_{in}\Omega$ is the circumferential speed of the inner cylinder surface, and $Re_d = U_{in}d/\nu$.

1.2. *A brief review of polymer drag reduction*

How polymers interact with turbulent flow to produce drag reduction is very much an open question. While there is agreement that polymer molecules elongate in drag-reducing flows, there is no consensus on how molecules elongate or the impact of this elongation on turbulence. One of the earlier drag-reduction hypotheses is described in Lumley (1969). He enumerated a number of important molecular parameters including molecular weight, flexibility, length, expansion, filamentation formation. He hypothesized that drag-reducing polymer molecules in turbulent boundary layers are stretched by the flow, resulting in an increase in the local fluid viscosity. This hypothesis was later reiterated by Hinch (1977), and others.

Hinch (1977) used physical arguments in conjunction with existing polymer elongation models to hypothesize a drag-reduction mechanism. He proposed that the elongation of a long-chain polymer molecule results in a dramatic increase in the viscosity of the fluid in the immediate vicinity of the molecule. The more the molecule stretches, the greater the increase in local viscosity. He concluded that the degree to which a molecule will elongate depends on the strain rate of the fluid surrounding the polymer.

A theoretical study was conducted recently by Rabin & Zielinska (1989). They examined the effect of polymer molecules on vorticity distribution in elongational flows. They began by pointing out that as long as the flow is Newtonian, vortex, stretching occurs over all wavenumbers. Their analysis showed that the addition of polymers inhibits the stretching of vorticity at high wavenumbers. Energy that would have been dissipated by small-scale vortices is transferred to and stored in extended polymer molecules. When the molecules advent into regions of low strain rate, they relax back into the natural state of a tangled ball. In so doing, the stored energy is returned to the low-wavenumber velocity fluctuations. Thus, Rabin & Zielinska (1989) argued, there will be a shift in the turbulent energy from high down to low wavenumbers.

There are equally convincing arguments, as represented by Massah *et al.* (1993), and Goldshtik, Zametalin & Shtern (1982), that elasticity of polymer molecules and not extensional viscosity is responsible for drag reduction. Massah *et al.* (1993) used a FENE bead spring model to develop insight into how polymers behave in turbulent flows. This was an extension of the work by Wiest, Wedgewood & Bird (1989) on extensional flows. While Massah *et al.* (1993) could not directly study turbulent boundary layers, they examined simple flows which had important characteristics of turbulence. One of the principal results of their study was that polymers will unravel in shear flows. They predicted that polymer elongation will therefore occur in the laminar sublayer, which is in direct contrast to arguments of Lumley (1969). They further point out that polymer elongation may not be a sufficient condition for drag

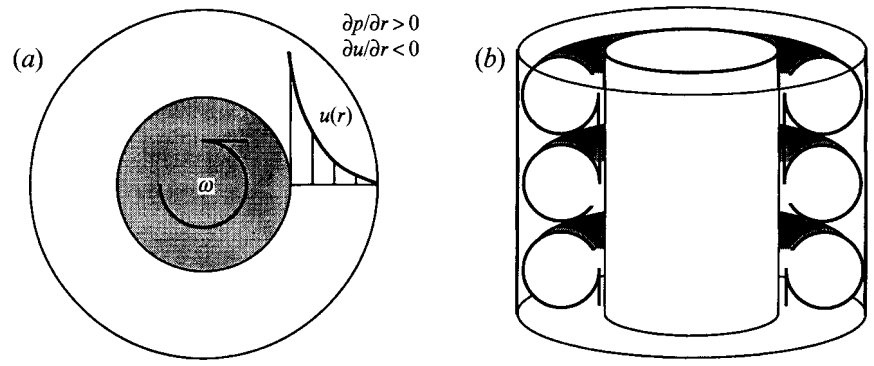

FIGURE 1. Top and radial section views showing the Taylor instability. The top view (*a*) shows the laminar circumferential velocity profile leading to the onset of Taylor vortices illustrated in (*b*).

reduction. As evidence, they cite experimental evidence of polymer elongation in laminar flow through a capillary tube with no measurable drag reduction.

Goldshtik *et al.* (1982) linearized the Navier–Stokes equations close to the wall in a turbulent boundary layer to model the effects of drag-reducing polymer additives. In modelling viscoelastic fluids, they assumed that the elastic terms would dominate the viscous terms. This led to predictions of mean and fluctuating velocities which agree quite well with experiments.

1.3. *Görtler vortices in Taylor–Couette flow*

Recently, Wei *et al.* (1992) experimentally examined small-scale structure in Taylor–Couette flow. They used laser-induced fluorescence (LIF) flow visualization techniques to show formation and evolution of counter-rotating streamwise vortices close to the inner cylinder wall. They argued that these vortices were the Görtler vortex phenomenon hypothesized by Smith & Townsend (1982) and Townsend (1984). Wei *et al.* (1992) further demonstrated that Görtler vortices forming the near-cylinder boundary layers were responsible for the herringbone structures reported by Fenstermacher, Swinney & Gollub (1979).

Development of Görtler vortices is shown schematically in figures 1 and 2. In this study, the outer cylinder is stationary. For low Taylor numbers, the mean velocity profile is sketched in figure 1 (*a*). Flow is entirely in the circumferential direction with a maximum at the inner cylinder. There is a radial momentum balance between the inertia of the fluid, which decreases with increasing radius, and the radial pressure gradient, which increases with increasing radius. When the Taylor number is greater than a critical value, Ta_{crit}, the inertia exceeds the pressure force and counter-rotating Taylor vortices are generated. These vortices are aligned in the circumferential direction and span the entire gap. This is shown in figure 1 (*b*).

Formation of Taylor vortices causes a redistribution in the mean circumferential velocity profile. Boundary layers are created at both the inner and outer cylinder walls. This is indicated in figure 2 (*a*). In the boundary layers, the same radial momentum balance exists. Inertia decreases with increasing radius while pressure gradient increases in a radially outward direction. Thus, at a sufficiently high Taylor number, smaller-scale counter-rotating vortices, Görtler vortices, will be generated in the boundary layers. This phenomenon was demonstrated by Wei *et al.* (1992) and is illustrated in figure 2 (*b*). There will be a range of Taylor numbers characterized by a hierarchy of circumferentially oriented vortices; small-scale near-wall vortices results from amplification and roll-up of Taylor–Couette instabilities.

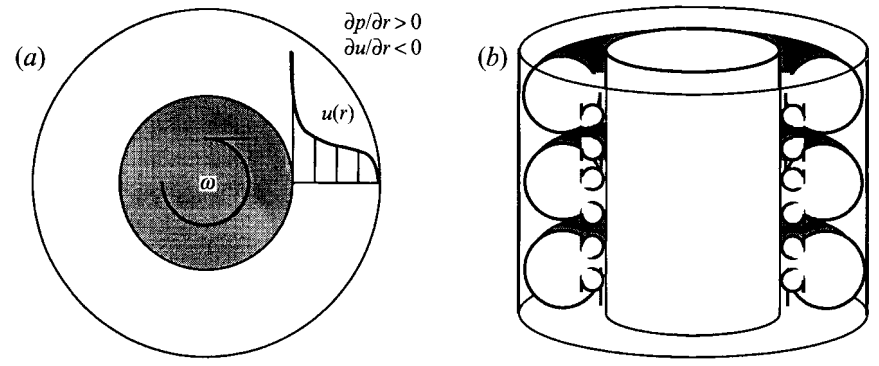

FIGURE 2. Top and radial section views showing the Görtler instability superimposed on the Taylor vortex flow. Taylor vortices redistribute the mean circumferential velocity profile (*a*) resulting in boundary formation which is subject to Görtler vortices (*b*).

1.4. *Objective*

It was noted at the outset that incomplete understanding of turbulent boundary layer instabilities prevents complete understanding of polymer drag reduction. While there are probably a number of dynamically significant instabilities in a turbulent boundary layer, one candidate for this list is the Görtler instability. In a series of publications, including Swearingen & Blackwelder (1987), Blackwelder hypothesized that near-wall streamwise vortices in plane turbulent boundary layer could be caused by amplification of Görtler instabilities at the solid boundary. This was based on an order of magnitude argument that even minute surface irregularities in a flat plate would be sufficiently large to generate Görtler vortices.

The approach taken in this paper is to examine the effect of polymers on a particular instability. Specifically, the question of whether or not drag-reducing polymer additives inhibit the growth of Görtler vortices is examined. Taylor–Couette flow is used because a hierarchy of near-wall inertial instabilities can be generated.

2. Apparatus

A Taylor–Couette experiment consisting of a circular inner cylinder rotating concentrically inside a stationary outer cylinder was constructed for this investigation. Premixed 'oceans' of dilute polyethylene-oxide (PEO) were used as working fluids in this study. The polymer was Polyox WSR-301, manufactured by Union Carbide, with molecular weight of approximately one million. Two flow visualization techniques, laser-induced fluorescence (LIF) and alumina particles, were used to examine the flow. A brief description of the cylinder assembly appears in the following paragraphs; the reader is referred to Wei *et al.* (1992) or Lee (1990) for greater detail. The flow visualization apparatus is listed in §3. A drawing of the apparatus appears in figure 3.

The outer cylinder was made from a 153.35 cm long section of clear Plexiglas pipe with an inner diameter of 30.28 cm. Two interchangeable inner cylinders were made from 152.40 cm lengths of Plexiglas pipe. The outer diameters measured 15.04 cm and 26.57 cm resulting in gap widths of 7.62 cm and 1.85 cm, respectively. In Wei *et al.* (1992), data from three inner cylinders were reported. The inner cylinders used in the present study were the medium and large cylinders (i.e. the medium and small gaps) and shall be referred to as such throughout the remainder of this paper. The cylinders were mounted on a 2.54 cm brass drive shaft which extended through the cylinder assembly.

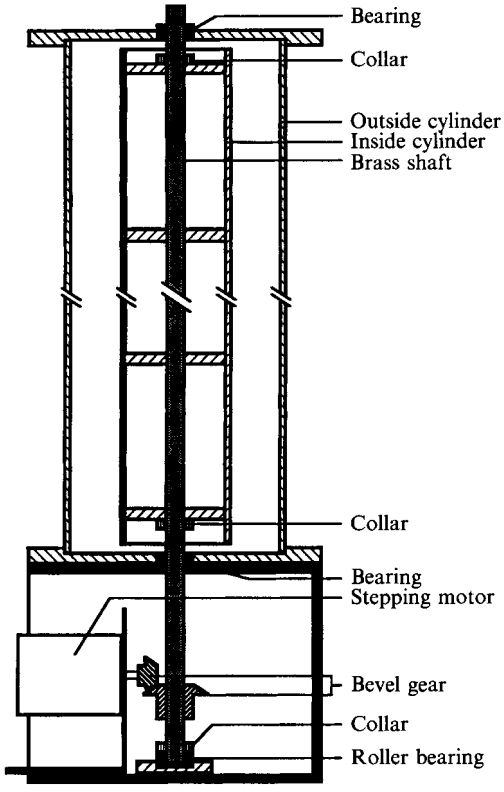

FIGURE 3. Schematic side view assembly drawing of the Taylor–Couette experiment.

The brass shaft was driven by a 25000 step per revolution microstepping motor and driver. Bevel gears with a 2:1 gear ratio were used to couple the motor output shaft to the brass inner cylinder drive shaft, as shown in figure 3. This resulted in the inner cylinders turning at a rate of one cylinder revolution per 50000 motor steps. A square wave generator was used as the input to the motor controller.

3. Experimental methods

3.1. *Flow visualization techniques*

Two different flow visualization techniques were used in this study. LIF was used to examine flow in the medium gap. Standard time exposure photography of alumina particles was used for the small gap. LIF studies were done using an Innova 70-4 argon ion laser operating in all-lines mode. The laser beam was aimed radially through the centre of the cylinders and spread into a vertical laser sheet by a 2.54 cm focal length cylindrical lens, illuminating the flow in the (r, z)-plane. This is shown in figure 4. The thickness of the sheet was ~ 0.2 cm. The advantage of this viewing orientation was that it was possible to see flow patterns close to the inner cylinder wall.

The fluid was marked with fluorescein dye injected upstream of the laser sheet using a syringe and a long 0.15 cm outer diameter stainless steel tube inserted between the cylinders through a hole in the top end plate. The most effective method of marking the flow close to the inner cylinder was to slowly bleed dye right on the surface of the inner cylinders and subsequently remove the injection tube. For the Taylor numbers

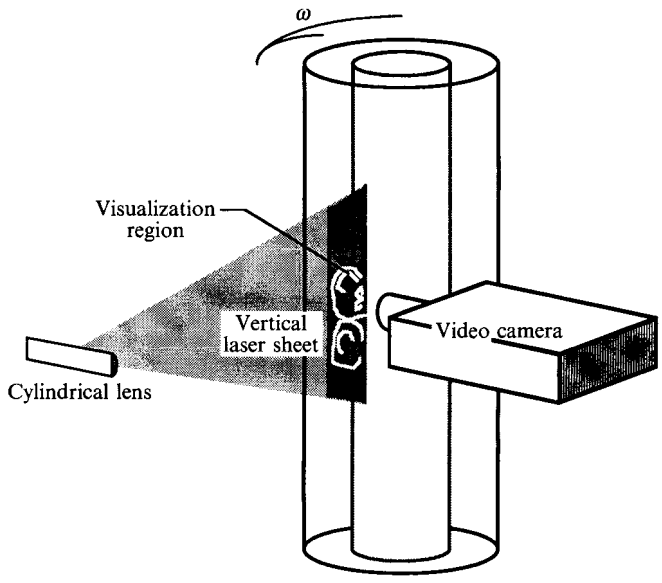

FIGURE 4. Oblique view drawing showing the LIF visualization apparatus and orientation.

examined, dye remained at the inner cylinder surface several minutes after the injection tube was withdrawn. Near-wall vortices would entrain dyed fluid away from the inner cylinder wall, making the vortices visible.

Visual records of the LIF experiments were made using a Sony professional quantity $\frac{3}{4}$ in. video system. This included a 3CCD colour camera, video recorder, and frame code generator. The $\frac{3}{4}$ in. system was equipped with variable slow motion and frame-by-frame playback. The video camera was positioned to view the entire gap. Orientations of the laser sheet and video camera are shown in figure 4. Because of the curvature of the cylinders, there were non-uniform refraction effects in the radial direction: objects close to the inner cylinder appeared larger than objects close to the outer cylinder. As long as the camera was far away from the cylinders, refraction effects in the axial direction were minimal.

3.2. *Quantitative analysis: measurement of the Görtler wavelength*

It was decided that the core-to-core separation distance between two counter-rotating vortices in a Görtler vortex pair should be measured in order to estimate the most unstable Görtler wavelength, which could be obtained by multiplying the core-to-core measurements by two. To improve the most unstable wavelength approximation, core-to-core measurements were made as soon as the pair was visible. Measurements were done with the aid of the reverse slow-motion playback feature of the video recorder. For a given Taylor number, the video was played until a counter-rotating vortex pair was seen. The tape was then reversed in slow motion playback until the vortex pair could just barely be identified. The video frame was then frozen and the core-to-core measurement was made. The location of a vortex core was generally identifiable as a small spot near the centre of the vortex which contained no dye. In certain instances the exact location of the cores was difficult to determine. The approximate centre of the vortex was used.

In order to account for the uncertainties in the core-to-core measurements, a number of independent measurements were made for each Taylor number. Wherever possible, a sample size of 20 to 25 different vortex pairs were examined for a given Taylor

number and gap size. Exceptions included the low Taylor number PEO cases: there were fewer measurements in a sample because polymers significantly decreased Görtler vortex formation. The mean and r.m.s. were computed for each ensemble, and a 95% confidence interval was computed assuming a Gaussian distribution.

3.3. *Experimental conditions*

A range of Taylor numbers spanning nearly three orders of magnitude was studied $3 \times 10^5 \leqslant Ta \leqslant 1 \times 10^9$; the range of parameters is shown in table 1. The critical Taylor number, Ta_{crit}, the centre column in table 1, refers to the lowest value of Ta at which Taylor vortices first appear. The value of Ta_{crit} for the medium gap was obtained by interpolating the results of Sparrow, Munro & Jonnsson (1964), and Walowit, Tsao & DiPrima (1964). The value for the small-gap case was based on experimental observations.

Two different concentrations of PEO, 20 and 100 p.p.m. (parts per million by weight), were examined along with the Newtonian baseline case, 0 p.p.m. The method of mixing PEO was similar to that described in Wei & Willmarth (1992). In brief, three 36 l drums were used to mix enough 100 p.p.m. solutions of PEO to fill the Taylor–Couette cylinders. Each drum was placed on a magnetic stirrer and filled with hot tap water. An appropriate amount of powdered PEO suspended in isopropyl alcohol was poured into the swirling water. The mixture was allowed to swirl for approximately 15 minutes before the drum was removed from the stirrer. The polymer solution was then allowed to hydrate in the drums for 24 h.

After 24 h had elapsed, the PEO solution was gently transferred to the Taylor–Couette experiment. When experiments called for 100 p.p.m., the contents of all three drums were transferred. In the case of the 20 p.p.m. experiments, the 100 p.p.m. PEO was diluted in the experiment. That is, four parts of water was added to the cylinder for every part of 100 p.p.m. PEO solution until the cylinder was filled. Obviously, for the baseline of 0 p.p.m., no polymer was used. Once the cylinder was filled, the polymer was allowed to hydrate for an additional 24 h to ensure that the polymer had thoroughly dissolved and become uniformly distributed throughout the experiment. Finally, on the morning of the experiment, the inner cylinder was turned at a speed greater than Ta_{crit} for several hours. Mixing by the Taylor and Görtler vortices eliminated any concentration gradients that may have existed due to settling of the polymer.

On the day of the experiment, the viscosity of PEO solutions were measured using a no. 50 Canon-Finske routine viscometer. The kinematic viscosities of the 20 and 100 p.p.m. PEO solutions were 0.0103 and 0.0113 $\mathrm{cm^2\,s^{-1}}$, respectively. This corresponds to intrinsic viscosities of 14.5 and 12.7. The intrinsic viscosity, η, is used as a measure of the age of the polymer solution and is defined as

$$\eta = c_{polymer}^{-1}\{(\nu_{polymer}/\nu_{solvent}) - 1\}, \tag{2}$$

where c is the polymer concentration in $\mathrm{g\,dl^{-1}}$, and $\nu_{polymer}/\nu_{solvent}$ is the ratio of kinematic viscosities of polymer solution and plain solvent.

It should be noted that, for the LIF studies, a small sample of test fluid was set aside prior to filling the Taylor–Couette experiment. Fluorescein dye (< 5 p.p.m.) was dissolved in this sample to ensure that the properties of the dyed fluid would closely match those of the test fluid. In so doing, it is possible that either the fluorescein degraded the polymer or the polymer inhibited the fluorescence of the dye. As a check, the pH of a 100 p.p.m. PEO solution was measured with and without fluorescein dye. The pH of PEO without dye was 7.36 while with fluorescein it was 7.45. (The pH of

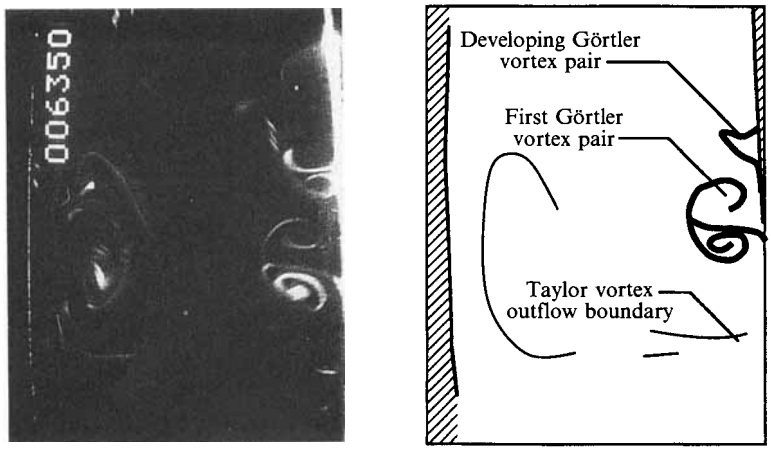

FIGURE 5. Still photograph and line drawing showing two representative Görtler vortex pairs. The photograph was taken from a medium-gap video record at $Ta/Ta_{crit} = 2128$. The inner cylinder is aligned with the right edge of the photograph; flow is out of the page.

Gap width, d (cm)	R_{in}/R_{out}	Aspect ratio (length/gap)	Ta_{crit}	Ta/Ta_{crit} range	PEO concentration (p.p.m. by weight)
1.85	0.88	82	1500	2×10^2–2×10^3	0 and 100
7.62	0.50	20	4700	2×10^3–2×10^5	0, 20 and 100

TABLE 1. Parameter range for the Taylor–Couette investigation. A range of Taylor numbers was examined with and without polymer additives for two different gap sizes. The critical Taylor number is defined in the text.

the local tap water was measured to be 6.63.) Because of the smaller difference in pH between dyed and undyed polymer, it is argued that fluorescein had little or no effect on the results presented in this paper. This conclusion is supported by the fact that independent flow visualization techniques (alumina particles) produced corroborating results.

4. Results and discussion

In this section, still photographs taken from LIF video sequences and alumina particle visualization experiments are shown to demonstrate the effect of polymer additives on the Görtler instability. In addition, measurements of the approximate Görtler instability wavelength are presented which quantitatively support the visual observations. A hypothesis is presented which explains the visual and quantitative results.

Figure 5 is a single still photograph showing two Görtler vortex pairs. This was taken from an LIF video sequence of the medium gap in which water was the working fluid. The accompanying schematic highlights the salient features in the photograph. The Taylor number is 1×10^7 which corresponds to $Ta/Ta_{crit} = 2128$. In the photograph, the laser sheet is in the plane of the page and the circumferential flow direction is out of the page. The video camera was oriented so that gravity acts from right to left. The inner cylinder appears as a bright white line along the right edge of

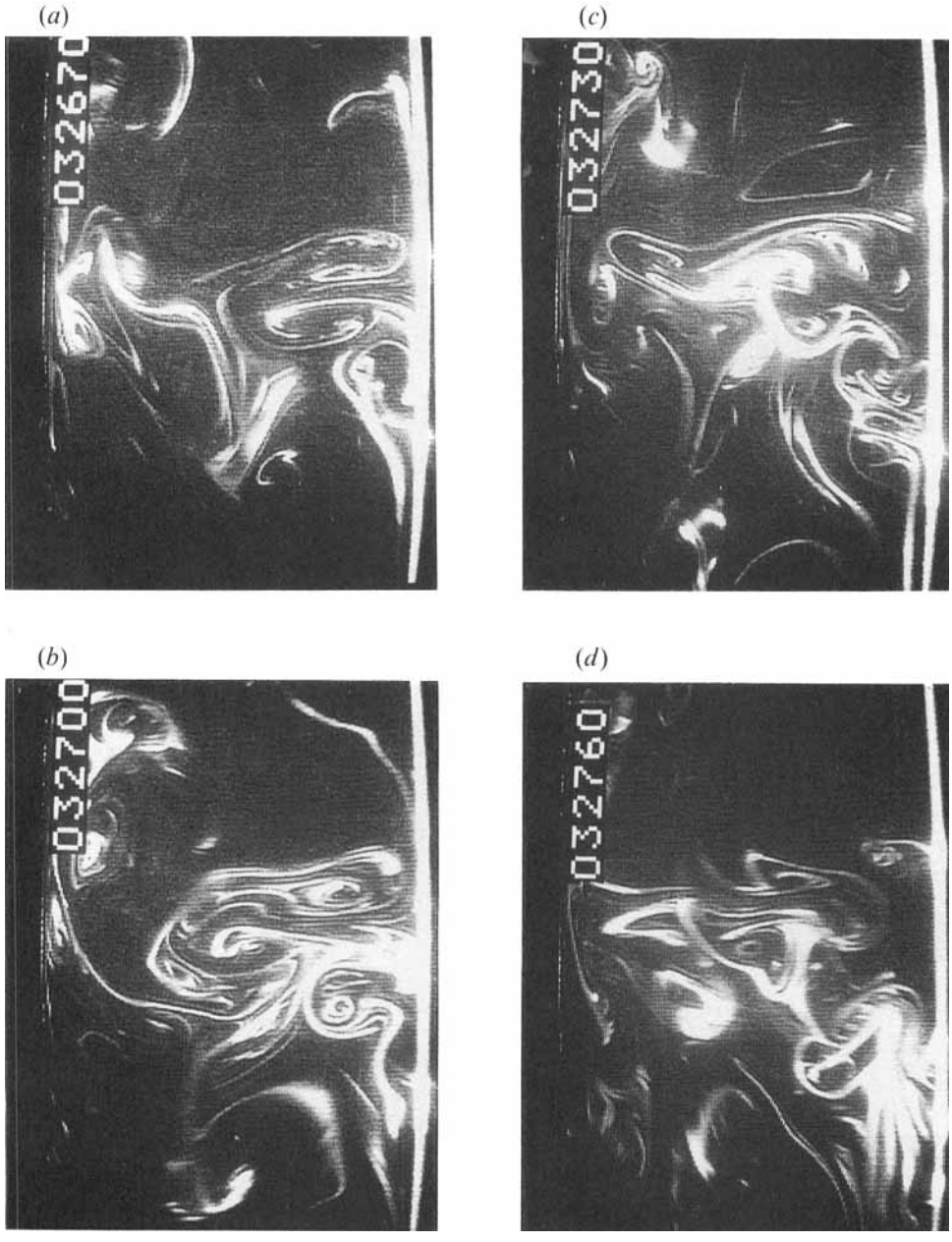

FIGURE 6. Still photograph sequence made from a medium-gap LIF video record of Newtonian flow at $Ta/Ta_{crit} = 6383$. The orientation is the same as in figure 5. Time elapse between successive photographs is 1.0 s.

the photograph while the stationary outer cylinder appears along the left. A detailed description of Görtler vortex formation and evolution in Taylor–Couette flows was presented in Wei *et al.* (1992).

Figure 6 is a sequence of four photographs showing Görtler vortices in the medium-gap case with water as the working fluid. The time lapse between successive photographs is 1.0 s; the photograph orientations are identical to figure 5. The Taylor

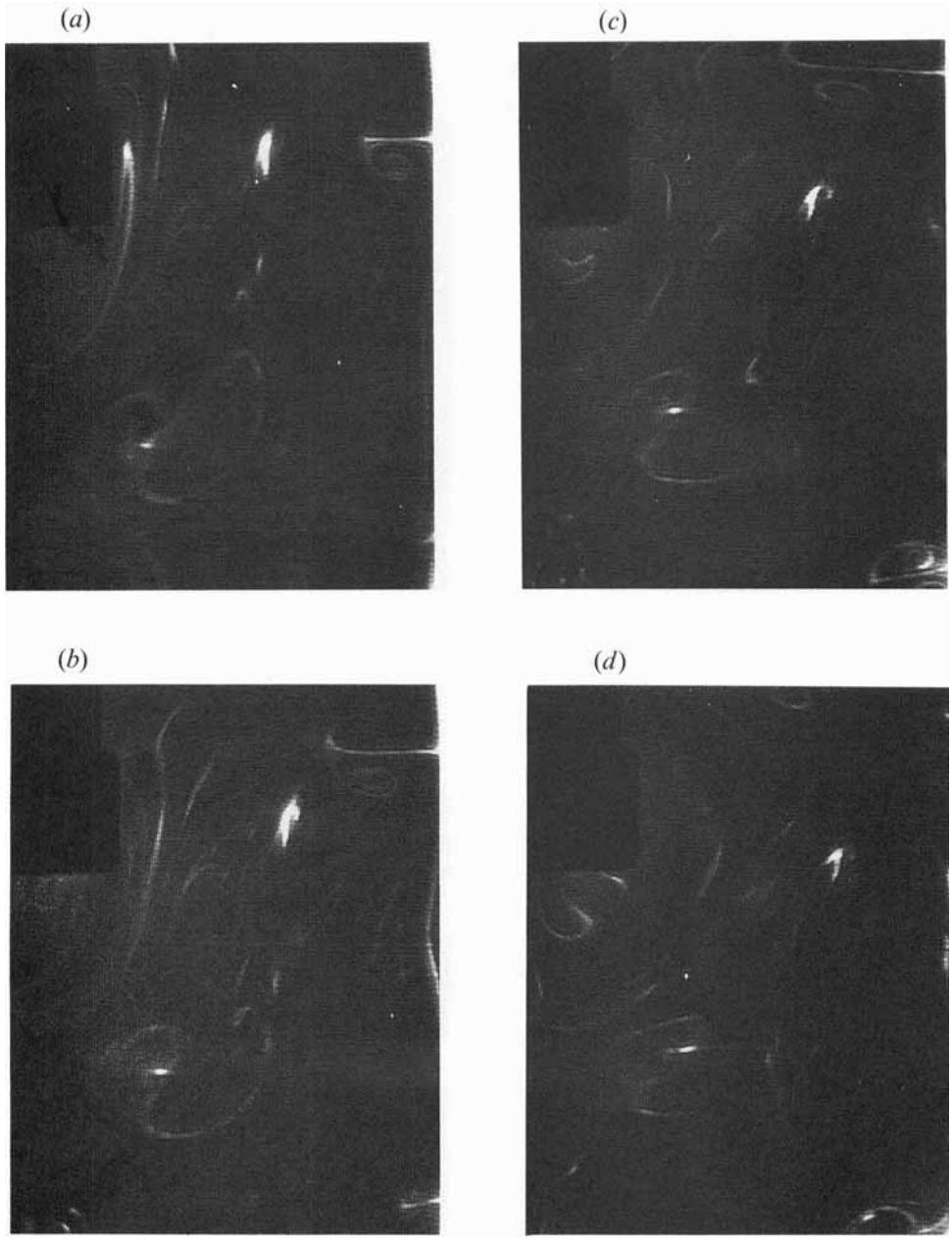

FIGURE 7. Still photograph sequence made from a medium-gap LIF video record of 100 p.p.m. PEO flow at $Ta/Ta_{crit} = 6383$. The orientation is the same as in figure 5. Time elapse between successive photographs is 1.0 s. Note the 'more laminar' appearance of the flow compared to the baseline case shown in figure 6.

number of this flow is 3×10^7 or $Ta/Ta_{crit} = 6383$. Note that a number of Görtler vortex pairs appear over the 4 s duration of the sequence. Also observe the 'turbulent' appearance of the dye in the gap.

By comparison, four still photographs appear in figure 7 for the same conditions except that the working fluid was a 100 p.p.m. PEO solution. Note that the inner cylinder was turned at a higher speed because the viscosity of the PEO solutions were

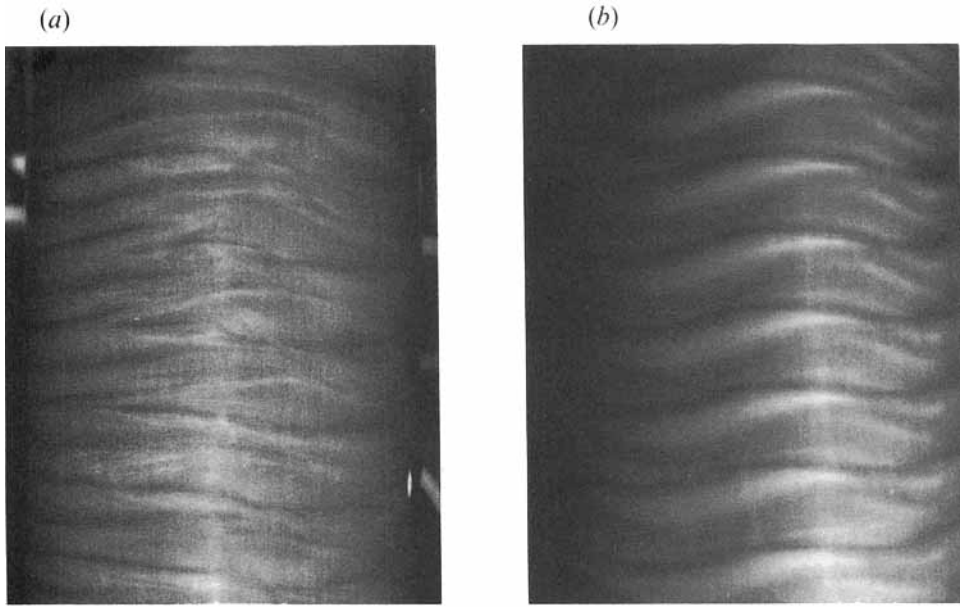

FIGURE 8. Alumina particle visualization photographs of the small gap at $Ta/Ta_{crit} = 200$: (*a*) Newtonian flow and (*b*) the 100 p.p.m. PEO case. Observe the 'turbulent spots' in (*a*) which are not present in (*b*).

higher than that of water. The higher speed was necessary to match Taylor numbers in water. The reader is also reminded that the fluorescein dye injected in the polymer cases was dissolved in a polymer solution identical in concentration to the test fluid.

The time lapse between successive photographs in figure 7 is again 1.0 s. Note the difference between figures 6 and 7. One Görtler vortex pair appears above centre in figure 7(*a–c*) and a second pair can be seen on the extreme bottom of Figure 7(*b–d*). The comparative lack of Görtler vortices in figure 7 suggests that the PEO suppresses Görtler vortex formation. The reduced picture quality in figure 7 resulted, in part, because injected dye diffused from the wall before any Görtler vortices formed. By contrast, Görtler vortices formed constantly in the water case, figure 6, and were therefore visible when there was still sufficient dye available to mark the vortices. It was also observed that the Görtler vortices in PEO, when they did appear, were larger and less energetic than their counterparts in water.

The fact that polymers affect Taylor–Couette flow at Taylor numbers which are not turbulent should not come as a great surprise in the light of previous works on the subject. A number of studies were conducted, including those of Giesekus (1972), Hayes & Hutton (1972), and Green & Jones (1982), to examine the effects of polymers on the onset of Taylor vortices. Each of these papers contain data indicating that polymers raise the critical onset Taylor number, Ta_{crit}. These studies were conducted at Taylor numbers orders of magnitude lower than this study.

Further visual evidence of the stabilizing effect of polymers on the Görtler instability appears in figures 8–10. Each of these figures is a pair of still photographs comparing flow in the small gap with and without polymer additives. The fluid in all photographs were seeded with fine alumina particles and illuminated with a floodlamp. Mean flow is left to right.

Figure 8 is a comparison of flows with and without PEO in the small gap at a Taylor number of 3×10^5; $Ta/Ta_{crit} = 200$. Figure 8(*a*) is the Newtonian baseline case, while

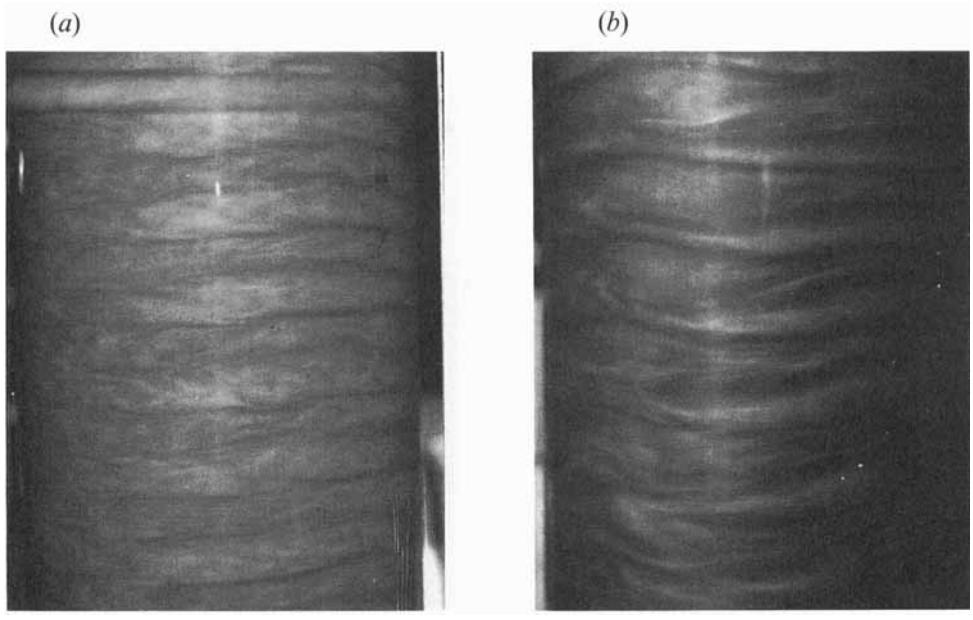

FIGURE 9. Alumina particle visualization photographs of the small gap at $Ta/Ta_{crit} = 667$; (*a*) Newtonian flow and (*b*) the 100 p.p.m. PEO case. Note the similarity between the polymer case in (*b*) and the lower Taylor number Newtonian case shown in figure 8(*a*).

figure 8(*b*) shows the flow of 100 p.p.m. PEO. In the Newtonian case, wavy Taylor vortices exhibit quasi-periodic 'turbulent spots' while the wavy vortices remain laminar in the polymer case.

At a higher Taylor number, $Ta = 1 \times 10^6$ or $Ta/Ta_{crit} = 667$, the stabilizing effect of polymers is again evident. This is shown in figure 9. Again parts (*a*) and (*b*) are the water and 100 p.p.m. PEO cases, respectively. Notice the 'herringbone' pattern in the Newtonian case. This was reported earlier by Fenstermacher *et al.* (1979) and recently explained in Wei *et al.* (1992) as Görtler vortices being advected by the large Taylor vortices to the outer cylinder. The corresponding polymer photograph, figure 9(*b*), bears a close resemblance to figure 8(*a*), the water case at a lower Taylor number.

This pattern continues at even higher Taylor numbers. Figure 10 shows photographs of flow between the small gap with and without polymers at $Ta = 3 \times 10^6$; $Ta/Ta_{crit} = 2000$. In figure 10(*a*), the Newtonian case, note the fine scale of the 'herringbone' patterns superimposed on the larger Taylor vortices. In contrast, the Görtler vortices are significantly larger in the 100 p.p.m. PEO case (figure 10*b*), which again bears a close resemblance to the lower Taylor number Newtonian case, Figure 10(*a*).

Variations in Görtler instability wavelength for different PEO concentrations are shown in figure 11. Tree PEO concentrations are shown; the baseline Newtonian case, 20 p.p.m. and 100 p.p.m. PEO Görtler instability wavelengths are non-dimensionalized by the inner cylinder radius and plotted as functions of Ta/Ta_{crit}. Error bars indicate 95% confidence intervals for each data set.

The salient features of figure 11 are that Görtler instability wavelength decreases with increasing Taylor number and with decreasing polymer concentration. The dependence of wavelength on Taylor number for the Newtonian case was the focus of Wei *et al.* (1992). The significant quantitative result of this paper is, for a given Taylor

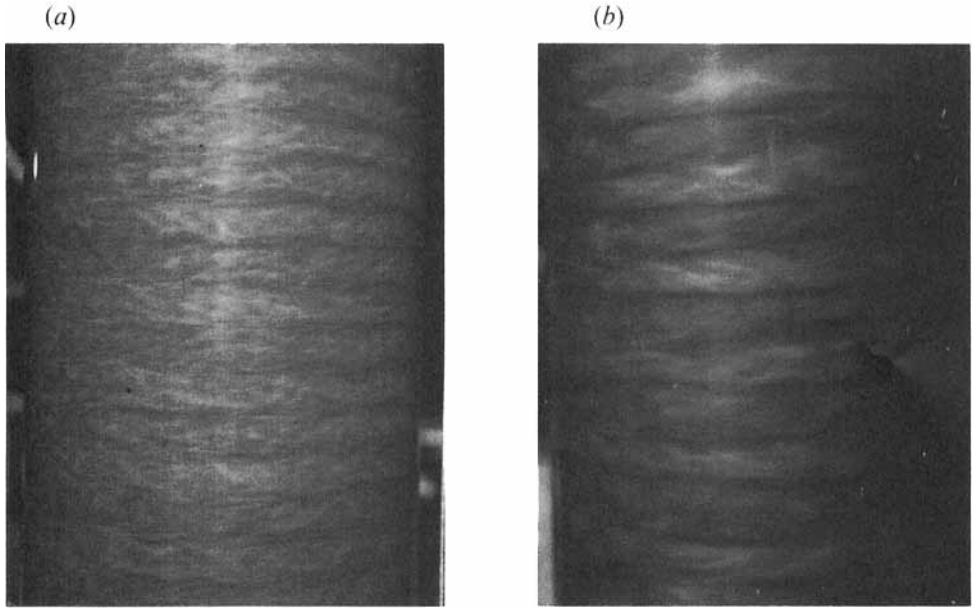

FIGURE 10. Alumina particle visualization photographs of the small gap at $Ta/Ta_{crit} = 2000$: (*a*) Newtonian flow and (*b*) the 100 p.p.m. PEO case. Again note that the polymer case appears less turbulent than the Newtonian case.

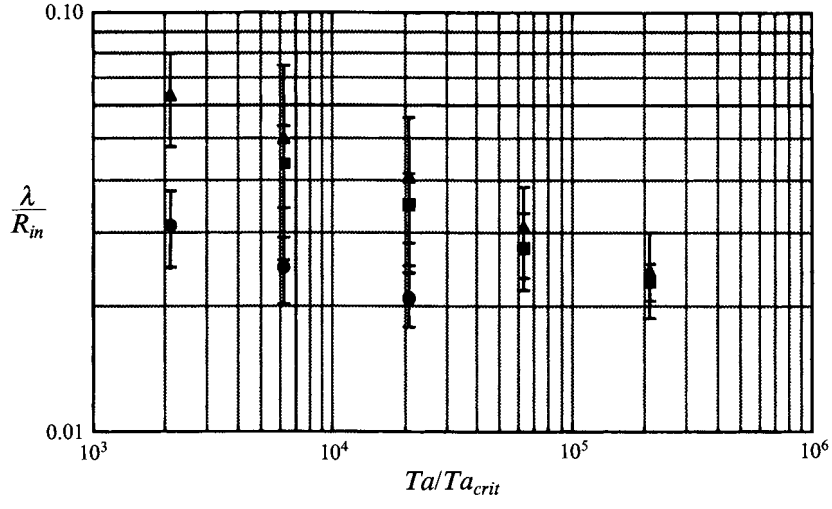

FIGURE 11. Görtler wavelength measurements for three polymer concentrations using the medium gap. Wavelength data are normalized by inner cylinder radius. Circles, squares, and triangles represent 0 (water), 20 and 100 p.p.m. PEO cases respectively.

number, that Görtler wavelength increases with increasing PEO concentration. This implies that polymers have a stabilizing effect on Görtler instabilities in Taylor–Couette flows.

As discussed in § 1.2, the role of polymers in drag reduction is still unresolved. One school of thought maintains that it is the *elasticity* of viscoelastic fluids that leads to drag reduction while others argue that *viscosity* is the dominant effect. If one subscribes to the theory that local increases in viscosity produce drag reduction, then the

stabilizing effect of polymers on Taylor–Couette flow can be explained with the following argument. First, there appears to be broader agreement that drag-reducing polymer molecules become elongated in flows with high strain rates. Further, Hinch (1977) proposed that this elongation results in a dramatic increase in the viscosity of the fluid in the immediate vicinity of the molecule. The more the molecule stretches, the greater the increase in local viscosity.

In Taylor–Couette flow, the region of highest strain rate is adjacent to the cylinder walls, particularly the inner cylinder wall. Taylor vortices redistribute the mean circumferential velocity profile creating regions of high mean shear close to the cylinder walls. This was shown in data from Townsend (1984) and was discussed in §1.3. Thus, polymer elongation occurs in regions where the flow is unstable to Görtler-type instabilities.

Since increased viscosity has a stabilizing effect on inertial instabilities, such as those found in Taylor–Couette flow, it can therefore be argued that PEO in the Taylor–Couette experiment increases viscosity close to the inner cylinder wall through elongation of polymer molecules. Further, this increased viscosity stabilizes the near-cylinder region thereby inhibiting formation of Görtler vortices. This is consistent with data in figure 11 and the visualization studies. The LIF sequences shown in figures 6 and 7 indicate that, for the same Taylor number, Görtler vortices formed in PEO are larger, less energetic, and appear less frequently than their counterparts in water. Finally, the increase in Görtler instability wavelength with increasing polymer concentration is demonstrated in figure 11.

In closing, it must be noted that a similar argument based on elasticity is more problematic. According to this hypothesis, introduction of PEO in the Taylor–Couette experiment introduces elastic term(s) that are responsible for stabilizing the flow. As pointed out by one of the reviewers, in certain instances, this elasticity term may be modelled as an increase in viscosity. However, this would not be the case in general.

5. Conclusions

Taylor–Couette flow at moderately high Taylor numbers with and without drag-reducing polymer additives (PEO) was examined using LIF and alumina particle flow visualization techniques. The objective of the study was to determine if polymers could inhibit the amplification and roll-up of inertial instabilities. Visual observations and measurements of the characteristic wavenumbers of Görtler vortices led to the conclusion that polymer additives do have a stabilizing effect on wall-bound centrifugal instabilities (i.e. Görtler vortex formation in Taylor–Couette flows). This effect can be explained by polymer molecule elongation in the high-strain field close to the cylinder walls which, in turn, results in a stabilizing increase in local viscosity. However, this hypothesis must be viewed with the understanding that there is no consensus on whether polymer drag reduction is controlled by elasticity effects or viscosity effects.

Supported under NSF Grant no. CTS-8909230.

REFERENCES

FABULA, A. G. 1966 An experimental study of grid turbulence in dilute high-polymer solutions. PhD dissertation, Dept. of Aero. Engng, Pennsylvania State University.

FENSTERMACHER, P. R., SWINNEY, H. L. & GOLLUB, J. P. 1979 Dynamical instabilities and the transition to chaotic Taylor vortex flow. *J. Fluid Mech.* **94**, 103.

GIESEKUS, H. 1972 On instabilities in Poiseuille and Couette flows of viscoelastic fluids. *Prog. Heat Mass Transfer* **5**, 187.

GOLDSHTIK, M. A., ZAMETALIN, V. V. & SHTERN, V. N. 1982 Simplified theory of the near-wall turbulent layer of Newtonian and drag-reducing fluids. *J. Fluid Mech.* **119**, 423.

GREEN, J. & JONES, W. M. 1982 Couette flow of dilute solutions of macromolecules: embryo cells and overstability. *J. Fluid Mech.* **119**, 491.

HAYES, J. W. & HUTTON, J. F. 1972 The effect of very dilute polymer solutions on the formation of Taylor vortices. Comparison of theory with experiment. *Prog. Heat Mass Transfer* **5**, 195.

HINCH, E. J. 1977 Mechanical models of dilute polymer solutions in strong flows. *Phys. Fluids* **20**, S22.

LEE, S. H.-K. 1990 The effect of drag reducing polymer additives on Taylor–Couette flows. MS thesis, Dept. of Mech. & Aero. Engng, Rutgers University.

LUMLEY, J. L. 1969 Drag reduction by additives. *Ann. Rev. Fluid Mech.* **1**, 367.

MASSAH, H., KONTOMARIS, K., SCHOWALTER, W. R. & HANRATTY, T. J. 1993 The configurations of a FENE bead-spring chain in transient rheological flows and in a turbulent flow. *Phys. Fluids* A **5**, 881.

RABIN, Y. & ZIELINSKA, B. J. A. 1989 Scale-dependent enhancement and damping of vorticity disturbances by polymers in elongational flow, *Phys. Rev. Lett.*, **63**, 512.

SMITH, G. P. & TOWNSEND, A. A. 1982 Turbulent Couette flow between concentric cylinders at large Taylor number. *J. Fluid Mech.* **123**, 187.

SPARROW, E. M., MUNRO, W. D. & JONSSON, V. K. 1964 Instability of the flow between rotating cylinders: the wide gap problem. *J. Fluid Mech.* **20**, 35.

SWEARINGEN, J. D. & BLACKWELDER, R. F. 1987 The growth and breakdown of streamwise vortices in the presence of a wall. *J. Fluid Mech.* **182**, 255.

TOWNSEND, A. A. 1984 Axisymmetric Couette flow at large Taylor numbers. *J. Fluid Mech.* **144**, 329.

WALOWIT, J., TSAO, S. & DIPRIMA, R. C. 1964 Stability of flow between arbitrarily spaced concentric cylinder surfaces including the effect of a radial temperature gradient. *Trans. ASME* E: *J. Appl. Mech.* **31**, 585.

WEI, T., KLINE, E. M., LEE, S. H.-K. & WOODRUFF, S. L. 1992 Görtler vortex formation at the inner cylinder in Taylor–Couette flow. *J. Fluid Mech.* **245**, 47.

WEI, T. & WILLMARTH, W. W. 1992 Modifying turbulent structure with drag reducing polymer additives in turbulent channel flows. *J. Fluid Mech.* **245**, 619.

WIEST, J. M., WEDGEWOOD, L. E. & BIRD, R. B. 1989 On coil-stretch transitions in dilute polymer solutions. *J. Chem. Phys.* **90**, 587.